Cytoplasmic hydrogen ion diffusion coefficient

Nabil F. Al-Baldawi and R. F. Abercrombie
Department of Physiology, Emory University School of Medicine, Atlanta, Georgia 30322 USA

ABSTRACT The apparent cytoplasmic proton diffusion coefficient was measured using pH electrodes and samples of cytoplasm extracted from the giant neuron of a marine invertebrate. By suddenly changing the pH at one surface of the sample and recording the relaxation of pH within the sample, an apparent diffusion coefficient of $1.4 \pm 0.5 \times 10^{-6}$ cm^2/s ($N = 7$) was measured in the acidic or neutral range of pH (6.0–7.2). This value is ~5× lower than the diffusion coefficient of the mobile pH buffers (~8×10^{-6} cm^2/s) and ~68× lower than the diffusion coefficient of the hydronium ion (93×10^{-6} cm^2/s). A mobile pH buffer (~15% of the buffering power) and an immobile buffer (~85% of the buffering power) could quantitatively account for the results at acidic or neutral pH. At alkaline pH (8.2–8.6), the apparent proton diffusion coefficient increased to $4.1 \pm 0.8 \times 10^{-6}$ cm^2/s ($N = 7$). This larger diffusion coefficient at alkaline pH could be explained quantiatively by the enhanced buffering power of the mobile amino acids. Under the conditions of these experiments, it is unlikely that hydroxide movement influences the apparent hydrogen ion diffusion coefficient.

INTRODUCTION

The diffusion coefficient of hydrogen and hydroxide ions and the intracellular buffering power determine how rapidly local changes in pH will be propagated. Within cells, the apparent diffusion coefficient determines, for example, whether standing gradients of pH can be maintained in acid-transporting epithelial cells (Aw and Jones, 1988) or whether transient pH gradients occur in localized regions of a muscle fiber (Irving et al., 1990). The theoretical treatment of pH gradients within cells is complicated, as both proton and hydroxide diffusion may need to be considered, and the diffusing protons may combine with mobile and immobile buffers. Junge and McLaughlin (1987) derived an expression for the effective diffusion coefficient for hydrogen ion, assuming that the pH is considerably more alkaline than the pK of both mobile and fixed buffers. Irving et al. (1990) derived the same expression with the less restrictive assumption that the changes in hydrogen ion concentration are small.

In this article, we report measurements of the apparent proton-hydroxide diffusion coefficient within the cytoplasm of the giant neuron of a marine worm (*Myxicola infundibulum*). In the pH range 6.0–7.2, we found a value ~1.4×10^{-6} cm^2/s. This, and the expected diffusion coefficient of cytoplasmic mobile buffers (~1×10^{-5} cm^2/s), suggests that ~15% of the cytoplasmic buffering power comes from mobile buffers and ~85% from immobile buffers. An observed increase in the diffusion coefficient to ~4×10^{-6} cm^2/s at pH 8.5 could be the result of increased buffering power of mobile amino acids.

The theoretical expression of Junge and McLaughlin (1987) and Irving et al. (1990), for the apparent diffusion coefficient, was extended to include hydroxide ion movement; to explore the applicability of this extended expression, a numerical simulation was done over the pH range of 5 to 9. This expression was used to define the conditions under which hydroxide ion movement would influence the proton–hydroxide diffusion coefficient.

METHODS

Experimental methods and procedures

The experimental set-up for our measurements is shown schematically in Fig. 1. The extracted cytoplasm from a giant neuron was aspirated into a glass capillary (~1 mm diameter). Two pH electrodes were placed in the sample, one with its tip at the surface of the cytoplasm and one inserted from the other end, its tip a measured distance (1–2 mm) from the surface. An indifferent voltage electrode was inserted from the distal end of the sample. From the start of the experiment, a solution of known pH was injected continuously to bathe the exposed proximal surface of the cytoplasm. The distal surface was exposed to air throughout the experiment. The voltage from each of the electrodes and the time were monitored by computer and stored on a 1.44 megabyte diskette. Each experiment included a calibration with known pH solutions so that the voltage reading could be converted to pH. Diffusion coefficients in cytoplasm, agar, or agar and bovine serum albumin ("artificial cytoplasm") were measured in the same manner.

0006-3495/92/06/1470/10 $2.00

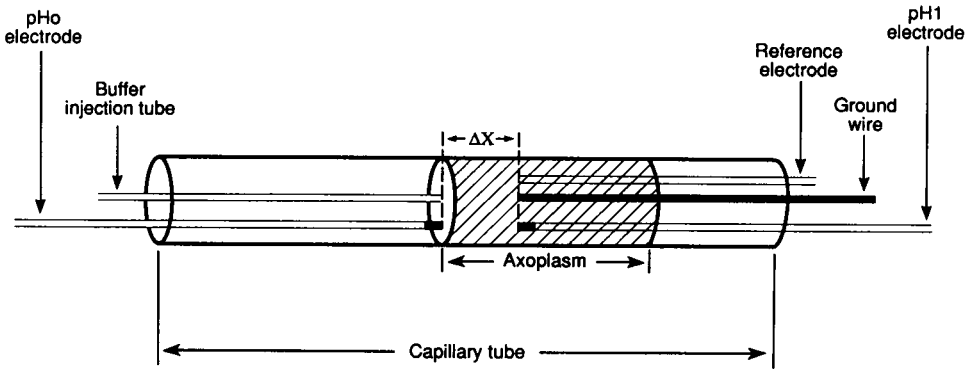

FIGURE 1 Schematic diagram of diffusion chamber. The axoplasm, represented as the shaded region, was placed in a glass capillary. Three electrodes were placed in the axoplasm. One pH electrode (pH_0) and the injector pipet were advanced from the left to the surface of the axoplasm. From the right, a second pH electrode (pH_1) and an indifferent voltage electrode were advanced. The distance from the surface to the second pH electrode (1–2 mm) was determined with a micrometer ruled to 0.025 mm. The experiment began with the injection of external buffer solution of a known pH into the vacant space adjacent to the axoplasm. This solution was continuously injected close to the surface of the axoplasm at a rate of ~100 μl/h. Temperature was 23°C.

Electrodes

The pH mini-electrodes were made of small plastic capillaries, 200–250 μm in diameter (Eppendorf GELoader™ tips; Brinkman Instruments, Inc., Westbury, NY). The electrodes were filled with a solution containing 300 mM KCl and 10 mM Hepes adjusted to pH 7. The electrode tips were plugged with a mixture of one part pH-sensitive resin (hydrogen ion ionophore I-Cocktail A; Fluka, Ronkonkoma, NY) combined with 0.2 parts polyvinyl chloride (PVC) and two parts tetrahydrofuran. We preferred plastic capillaries to the customary glass capillaries because the resin made a tighter seal with plastic. The plastic electrodes were also more stable and less prone to damage. The sensitivity of the pH electrodes, after overnight equilibration, was 56–58 mV per pH unit over the range, pH 5–9. When quickly transferred from one calibrating solution to another, the change in potential was typically 80% complete within 10 s.

Preparation

Neural cytoplasm was extracted from the giant axon of the marine annelid *Myxicola infundibulum* as previously described (Abercrombie and Hart, 1986). The gel-like consistency of this material was ideal for studying diffusion; it did not allow mixing or bulk flow of the diffusing substance. As a control, 3% agar or a mixture of 3% agar and BSA were dissolved in warm buffer solutions that had been precalibrated at room temperature to pH 7. Then the agar was allowed to solidify in glass capillaries to form "artificial axoplasm."

Solutions

The external buffer solutions contained 180 mM glycine, 116 mM L-cysteic acid, and 75 mM aspartic acid (Table 3) and were adjusted to pH 5–9 with HCl or KOH. This buffer composition is similar to the free amino acid composition of *Myxicola* axoplasm (Gilbert, 1975). These solutions were used to calibrate the pH electrodes; they were also added to the surface of axoplasm samples to change the pH suddenly for determination of hydrogen ion diffusion coefficients.

Analysis of data

The computer-assisted analysis was done in the following steps. (*a*) The voltages from the electrodes were converted to pH by comparing their values in unknown media to their values in known reference solutions. (*b*) The hydrogen and hydroxide concentration, and the quantity $[H^{+-}] = [H^+] - [OH^-]$, were computed for each recorded point. A diffusion coefficient can be calculated using either $[H^+]$, $[OH^-]$, or $[H^{+-}]$ (see Appendix). $[H^{+-}]$ was used for mathematical convenience and to insure that the calculations were not biased at high or low values of $[H^+]$ or $[OH^-]$. (*c*) A ratio, R, was then calculated according to Eq. 1 following Crank (1985). In Eq. 1, $[H^{+-}]_0^{fin}$ corresponds to the final reading from the surface pH electrode after adding the new buffer, $[H^{+-}]_1^{init}$ corresponds to the reading from the internal pH electrode before adding the new buffer, and $[H^{+-}]_1$ corresponds to the reading from the internal electrode at any time after adding the new buffer.

$$R = \frac{[H^{+-}]_1 - [H^{+-}]_1^{init}}{[H^{+-}]_0^{fin} - [H^{+-}]_1^{init}}. \quad (1)$$

During an experiment, the ratio, R, progresses from an initial value of zero toward a final value of one. The effective diffusion coefficient, D', is then calculated as:

$$R = erfc(x/2\sqrt{(D't)}), \quad (2)$$

where x is the distance from the surface to the pH_1 electrode, t is the elapsed time from the beginning of the injection, and *erfc* is the error-function complement [$erfc(x) = 1 - erf(x)$]. Since R, x, and t are known, D' can be calculated for each time point of the experiment by making use of a table of values of the error-function complement, $R = erfc(z)$ (Crank, 1985). By using Eq. 2, we assume a semi-infinite length of axoplasm. The actual length was ~0.5 cm. The more accurate expression for a finite length, L, of axoplasm may be derived using the method of images and a reflecting boundary at $x = L$.

$$R' = erfc(x/2\sqrt{(D't)}) + erfc((2L - x)/2\sqrt{(D't)}). \quad (3)$$

On the right-hand side of Eq. 3, the size of the second term compared with the first is an estimate of the error introduced by assuming a semi-infinite medium. Choosing typical values of $D' = 10^{-5}$ cm²/s, L =

0.5 cm, x = 0.1 cm, and t = 5,000 s; the second term in Eq. 3 is less than 0.005, the first term is ~0.75.

The calculated value of D' is a very sensitive function of the voltage of the pH_1 electrode when R is above 0.6 and below 0.2. To minimize the experimental error in our determinations, only values of R between 0.2 and 0.6 were used to calculate D'.

Titrations

Potentiometric titrations were done of suspensions of axoplasm, of solutions of the external buffer, and of solutions of BSA. The buffering power was calculated as the amount of HCl or KOH needed to change the pH of a liter of material (axoplasm, external bufer, or BSA solution) by one unit. The total buffering power is the sum of the buffering power of all groups that bind protons. The buffering power, β, contributed by any particular proton binding group with known pK and concentration C is given by

$$\beta \approx \frac{C \ln (10) 10^{-(pK + pH)}}{(10^{-pH} + 10^{-pK})^2} \quad (4)$$

(see Roos and Boron, 1981).

Numerical methods

In the Appendix, two approximations will be made to derive an analytical expression for the effective proton–hydroxide diffusion coefficient. To explore the regions and the deflections of pH under which these approximations are justified, the diffusion problem was solved by finite-difference methods. A diffusion region of 625 μm length was divided into 25 elements, each 25 μm in length. The model contained a mobile and a fixed pH buffer of defined concentrations and dissociation constants. The first step of the finite-difference simulation was to set the basal pH, which determined the starting concentration of hydrogen and hydroxide ions and the level of saturation of the fixed and mobile buffers. To begin the simulation, the pH at the origin was changed to a new value. For each time step (20 ms in our simulations), the finite-difference approximation of the linear diffusion equation (5) was used to calculate the movement of hydroxide ion, hydrogen ion, and protonated mobile buffer among the 25 elements (I = 1–25) (see Crank, 1985).

$$\Delta Q_k(I) = D_k * \Delta T * (Q_k(I + 1) - 2 * Q_k(I) + Q_k(I - 1))/(\Delta X)^2, \quad (5)$$

where $Q_k(I)$ is the concentration at each element (I) of the mobile material, k, under consideration, $\Delta Q_k(I)$ is the change in concentration for each time step, D_k is the diffusion coefficient of the mobile material (H^+, OH^-, or mobile buffer), ΔT and ΔX are the time step and element size of the computer simulation. A reflecting boundary is assumed at the 25th element. Next, the redistribution of protons among the mobile and fixed buffers at their new equilibria was computed for each of the 25 elements. There are several iterative methods that can accomplish this; however, for rapid convergence, we have found that solving the cubic equation for free protons using Newton's iterative procedure works well (Abercrombie, 1988). After the free hydrogen ion concentration is calculated, the new concentrations of the protonated mobile and immobile buffers are computed. To correct for cumulative errors, the total proton concentration in each element was checked to ensure conservation of mass. Finally, the reaction between hydrogen and hydroxide ions is allowed to take place. After a number of iterations (usually 800), a diffusion profile is generated. The apparent diffusion coefficient was computed for elements 2–24 using Eq. 5 and the change in $[H^{+-}]$ for the final two time steps. These values were then averaged over a region within the simulated sample.

EXPERIMENTAL RESULTS

Fig. 2 *A* shows a typical experiment in which the pH at the edge of an axoplasm sample was deflected from its basal value of 7.74 to a value of 9. Initially, the pH electrodes were placed in calibrating solutions of pH 7 and 9, and then allowed to equilibrate in the axoplasm for 10 to 25 min. Once the electrodes began to record a steady pH, the pH 9 solution was injected into the vacant space adjacent to the sample at c, resulting in the rapid change of the voltage of the surface electrode (V_0). The voltage of the inner electrode (V_1) changed more slowly as a result of the greater diffusion delay to the V_1 electrode tip. The diffusion coefficient calculated from these data (see Methods) is shown in Fig. 2 *B*.

In a series of experiments, the axoplasm pH was shifted to both acidic and alkaline values, and the diffusion coefficient determined over a range of pH. Results are shown as open squares in Fig. 3. The higher values determined for the effective hydrogen ion diffusion coefficient at alkaline pH can be quantitatively explained by the increase in the buffering power of the mobile amino acids (see Discussion).

To evaluate this method, experiments were done with "artificial axoplasm" made with 3% agar dissolved in the external buffer solution (pH 7), or with a mixture of 3% agar and BSA dissolved in the external buffer solution. In Fig. 3, the diffusion coefficients in the two types of artificial axoplasm (with and without BSA) were included with the coefficients in axoplasm to illustrate the influence of immobile and mobile buffers as described by Junge and McLaughlin (1987) and Irving et al. (1990). When BSA was added to the agar, the apparent hydrogen ion diffusion coefficients dropped, but not to the values measured with *Myxicola* axoplasm.

BSA was added to the "artificial axoplasm" to simulate an immobile buffer. Although the diffusion coefficient of BSA is not zero, it is at least twenty times lower than that of the amino acids (Table 1). Because the buffering power of 3% BSA and the buffering power of the external solution of mobile amino acids are comparable while the BSA diffusion coefficient is much lower, a reasonable approximation is to assume that BSA is immobile. (See Appendix Eq. A10 and Fig. 4.)

A 3% agar gel made up in the amino acid buffer contains ~97% water and therefore should, in principle, form an ideal convection-free aqueous environment for diffusion measurements. This assumes that protons and mobile amino acids do not interact with the polysac-

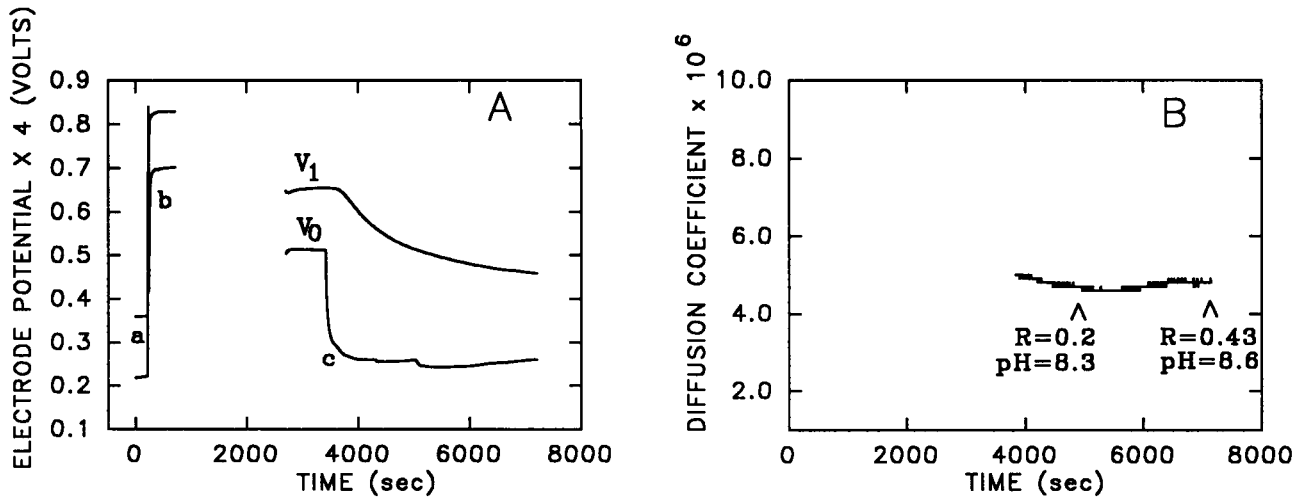

FIGURE 2 Determination of diffusion coefficient in axoplasm. (*A*) Voltage of each of the pH-sensitive electrodes relative to the potential of the indifferent electrode. The two traces represent two electrodes with different absolute voltage readings. The electrodes were first placed in standard solutions of pH 9 and 7 (at times *a* and *b*) before being placed in the axoplasm. Axoplasm pH for this experiment was 7.74. At time *c*, the experiment was begun by injecting an external buffer solution of pH 9 into the space adjacent to the axoplasm. (*B*) The diffusion coefficient calculated from this record with Eq. 2.

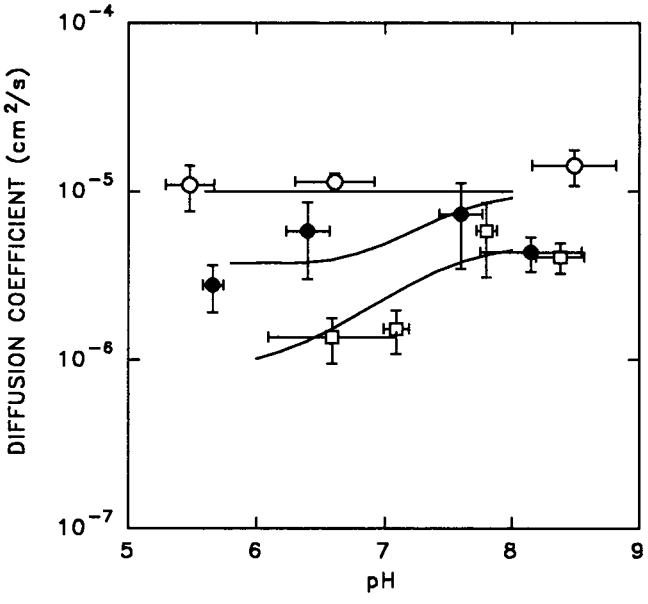

FIGURE 3 Diffusion coefficients. In amino acid buffer solution (Table 3) with 3% agar (*open circles*); in amino acid buffer solution containing 3% BSA and agar (*filled circles*); in neural cytoplasm (*open squares*). The vertical bars represent plus and minus one standard error. The horizontal bars represent the pH range over which the diffusion coefficient was determined. The lines were drawn according to the equation $D^{app} = D_M^{aq}\,\beta_{mob}/(\beta_{mob} + \beta_{immob})$ of Irving et al. (1990) using measurements of β_{mob} and β_{immob} shown in Fig. 4.

charide chains of the gel. If these interactions are minimal, we should measure, in the artificial axoplasm lacking BSA, an apparent H^+ diffusion coefficient equal to that of the free amino acids. Data shown in Table 2 and Fig. 3 are well described by assuming a diffusion coefficient of the mobile buffer of 1×10^{-5} cm^2/s, which is near that of the mobile amino acids of the external medium (see Table 1).

TABLE 1

Buffer	MW	Diffusion coefficient (25°C) Estimated*	Measured
		$\times 10^6\,cm^2\,s^{-1}$	
Glycine	75	10.6	10.6‖
Cysteic acid	169	7.1	6.3‡
Aspartic acid	133	8.0	
$MgATP^{-2}$	532	4.0	
Na_2ATP^{-2}	553	3.9	4.0§
H_3PO_4	98	9.3	9.4¶
$H_2PO_4^-$	97	9.3	8.8**
HPO_4^{-2}	96	9.4	
H_3O^+	19		93‖
OH^-	17		53‖
BSA	67,000	0.35	0.66‖

*Using $D \times (MW)^{1/2}$ = constant and glycine as reference. ‡McBain (1944). §Bowen and Martin (1964). ‖Longsworth (1954). ¶Edwards et al. (1966). **Mason and Culvern (1949).

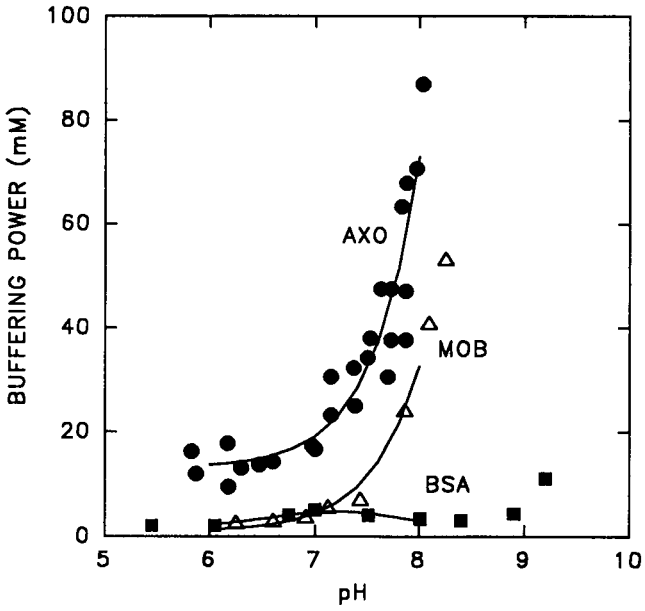

FIGURE 4 Buffering power. Axoplasm (AXO) buffering power was determined by titrating a mixture of 17.3 μl of axoplasm and 82.7 μl of 300 mM KCl with HCl and KOH as described by Spyropoulos (1960) (*filled circles*). Buffering power increased in the alkaline pH range. External buffer solution (MOB) titrated with HCl and KOH (*open triangles*). BSA disolved in deionized water and titrated with HCl and KOH (*filled squares*). The lines were drawn according to the semi-emperical equation $\beta = 2.3\,C\,10^{-(pH+pK)}/(10^{-pH} + 10^{-pK})^2 + B$. Best fit parameters were as follows: AXO, C = 2306 mM, pK = 9.9, B = 13.1 mM; MOB, C = 400 mM, pK = 9.4, B = 1.1 mM; BSA, C = 5.6 mM, pK = 7.2, B = 1.6 mM.

TABLE 2

	pH range	Diffusion coefficient* ± SEM
Sample (jump)		($cm^2/s \times 10^6$)
Agar		
pH 5	5.66 – 5.29	10.9 ± 3.3
pH 6	6.92 – 6.30	11.4 ± 1.4
pH 9	8.16 – 8.82	14.2 ± 3.4
Agar + BSA		
pH 5	5.74 – 5.58	2.8 ± .48
pH 6	6.57 – 6.23	6.88 ± 3.1
pH 8	7.43 – 7.76	7.32 ± 3.9
pH 9	7.95 – 8.53	4.33 ± .56
Axoplasm		
pH 5	7.12 – 6.05	1.36 ± .24
pH 6	7.16 – 7.02	1.52 ± .44
pH 8	7.75 – 7.88	5.82 ± 2.75
pH 9	8.19 – 8.57	4.07 ± .83

*Calculated from pH relaxation measurements using values of $0.2 < R < 0.6$.

Irving et al. (1990) have given a useful expression for calculating the effect of mobile and immobile buffering power on the apparent hydrogen ion diffusion coefficient.

$$D^{app} = D_M^{av} \frac{\beta_{mob}}{\beta_{mob} + \beta_{immob}}, \quad (6)$$

where D^{app} is the apparent hydrogen ion diffusion coefficient, D_M^{av} is the weighted average diffusion coefficients of the mobile buffers, β_{mob} and β_{immob} are the mobile and immobile buffering powers.

We assume an average diffusion coefficient of the mobile buffers, D_M^{av}, of 1×10^{-5} cm/s. Because the diffusion coefficients of plausible cytoplasmic mobile buffers are similar (Table 1), the identity of the mobile buffer within the cytoplasm is of little importance for our purposes. Buffering power for the mobile and immobile buffers of the axoplasm (β_{axo}), for the external buffer solution (β_{mob}), and for 3% BSA (β_{BSA}) are shown in Fig. 4.

Over the pH range of 6–8, β_{BSA} varied between 2–4 mM with the maximum of 4 mM near pH 7. Above pH 8.5, β_{BSA} began to increase, reaching ~10 mM at pH 9. The buffering power of the mobile amino acids of the external solution (β_{mob}) was ~2 mM over the pH range of 6–7 and increased steeply above pH 7 to a value near 50 mM at pH 8. This rise in the buffering power at alkaline pH is the result of free amino groups of the amino acids (see Table 3). The buffering power of *Myxicola* axoplasm was ~15 mM from pH 6–7 and increased steeply to between 60–80 mM at pH 8. These values for *Myxicola* are nearly identical to those determined for the axoplasm of squid (Spyropoulos, 1960; Boron and De Weer, 1976). The rise in buffering power at alkaline pH is consistent with the results of Spyropoulos (1960) and the free amino acids that were found in *Myxicola* axoplasm by Gilbert (1975).

The theoretical lines shown in Fig. 3 were drawn according to Eq. 6 using the estimates of β_{mob} and β_{immob} from the best-fit curves of Fig. 4. Therefore, the pH dependence of the apparent hydrogen ion diffusion coefficients is consistent with the pH dependence of the buffering power of the mobile amino acids. Only the data point representing agar-BSA-saline with the jump to pH 9 appears to be far off the line described by Eq. 6.

DISCUSSION

The apparent proton–hydroxide diffusion coefficient at pH 6.0–7.2 is $1.4 \pm 0.5 \times 10^{-6}$ cm²/s. That the diffusion coefficient is lower than ~1×10^{-5} cm²/s (the expected

TABLE 3

Buffer*	pK§	Concentration‡	d[HM]/d[H⁺] Max	pH6	pH7	pH8
		mM				
Glycine	2.3	180	36	36	36	36
	9.6		7×10^8	45	4,500	43×10^4
L-cysteic acid	2	116	12	12	12	12
	8.7		6×10^7	230	2.2×10^4	1.6×10^6
	12.7		6×10^{11}	0.02	2.3	231
Aspartic acid	2	75	8	8	8	8
	3.7		376	372	375	375
	9.6		3×10^8	19	1,900	18×10^4
$MgATP^{2-}$	4.6	~1	40	37	39	40
HPO_4^{2-}	2	~1	0.1	0.1	0.1	0.1
	6.8		6,300	118	2,400	5,600
	12		10^9	0.001	0.1	10
		Total d[HM]/d[H⁺]		877	3.1×10^4	2.2×10^6
		Total β_M (mM)		2	7.2	51

*Mobile cytoplasmic buffers. ‡Amino acid composition of *Myxicola* axoplasm from Gilbert (1975). §Martell and Smith, 1974; Dawson et al., 1986.

mobile buffer diffusion coefficient) can be explained using Eq. 6 by assuming a greater proportion of immobile buffer (81–91%) to mobile buffer (9–19%). We found that elevating the pH to 8.5 gave higher values of the diffusion coefficient suggesting a pH dependence of this parameter.

pH dependence of the diffusion coefficient

We examined two possible explanations for the rise in the diffusion coefficient at alkaline pH. First, we considered whether hydroxide movement might contribute disproportionately at high pH. From Appendix Eqs. A9–A12, it is possible to define the conditions under which hydroxide movement will be important: if the term on the left of Eq. 7 is similar to or greater in magnitude than the terms on the right.

$$D_{OH^-}\{10^{-14}/[H^+]^2\} \geqq D_M\{d[HM]/d[H^+]\}$$
$$= D_M\{\beta_M/[H^+] \ln (10)\}. \quad (7)$$

D_{OH^-} and D_M are the diffusion coefficients of hydroxide and mobile buffers, $[H^+]$ is the hydrogen ion concentration, [HM] is the concentration of the mobile buffer, and β_M is the buffering power of the mobile buffer (see Appendix).

If we take $D_{OH} = 10^{-4}$ cm²/s and $[H^+] = 10^{-8}$ (pH 8), then the term on the left of Eq. 7 has a value of 0.01. The term on the right will depend on the mobile buffer diffusion coefficient D_M and the buffering power of the mobile buffer. We assume ~400 mM amino acid for the mobile buffer. At pH 8, $d[HM]/d[H^+] \approx 10^6$ (see Table 3). Using 10^{-5} cm²/s for D_M, the term on the right of Eq. 7 has a value of 10. It is unlikely, therefore, that the hydroxide contribution will overtake the contribution of the mobile amino acids of this preparation. The reason for concluding that OH^- diffusion does not contribute significantly even at pH 8.2–8.6 is that the mobile buffer capacity becomes so large in this pH range. Since for this preparation OH^- is not a major contributor to D_{app}, the theoretical treatments of Junge and McLaughlin (1987) or Irving et al. (1990) are equally adequate for *Myxicola* axoplasm as the treatment given in the Appendix, which includes OH^-. The hydroxide contribution might, however, become significant at pH 8 in other systems where the mobile buffers are present in low concentrations or if they do not have pKs in the 8–10 range.

A more likely explanation for the rise in the apparent diffusion coefficient in *Myxicola* axoplasm is the increased buffering power of the mobile buffers. Eq. 6 from Irving et al. (1990) describes the contribution of mobile buffers. Because the diffusion coefficient did not change greatly over the acidic or neutral pH range, we conclude that the ratio of $\beta_{mob}/\beta_{immob}$ remains relatively constant in this range, i.e., β_{mob} and β_{immob} must have the same dependence on $[H^+]$. As the pH rises above 7, β_{mob} might increase more rapidly than β_{immob} as a result of the

free amino groups of the mobile amino acids. According to Eq. 6, an apparent hydrogen ion diffusion coefficient of 4×10^{-6} cm^2/s and a mobile buffer diffusion coefficient of 10×10^{-6} cm^2/s suggests that ~40% of the total buffering power results from the mobile buffers. This increase in the proportion of mobile buffer power is consistent with the measurements shown in Fig. 4. Although this explanation has not been proven, the contribution of hydroxide movement to the measured increase in D^{app} seems to be unlikely in this system.

Assumptions regarding hydroxide binding to metal ions

The theoretical expressions that we used for the apparent proton–hydroxide diffusion coefficient (Appendix) assumes that hydroxide ions do not attach to mobile or immobile sites within the cell. At alkaline pH, hydroxide metal ion pairs may form. Of the metal ions present within a cell, Mg^{+2} and Ca^{+2} are most likely to form pairs with OH^- (Smith and Martell, 1981). Using hydroxide metal ion stability constants and values for free magnesium of 3 mM (De Weer, 1976) and free calcium of 0.1 μM (Baker and Schlaepfer, 1978) yields $[MgOH]/[OH^-] = 0.21$ and $[CaOH]/[OH^-] = 4.4 \times 10^{-7}$. We conclude that the movement of hydroxide metal ion pairs will be small compared with the movement of hydroxide.

Evaluation of method and sources of error

We believe the principal source of error results from the mechanics of performing these experiments. For example, if the plug of agar or the axoplasm were forced to move when the solution is injected, then the diffusion distance might decrease. Or, if the injected solution were able to move by capillary action between the sample and the surrounding glass tube, then bulk flow and diffusion could influence the pH changes. These errors would increase the apparent diffusion coefficient. The measured diffusion coefficient in agar of $1.1 \pm 0.3 \times 10^{-5}$ cm^2/s compares favorably, however, with the diffusion coefficients of the mobile buffers, $0.7–1.0 \times 10^{-5}$ cm^2/s (Table 1), suggesting that this method gives a reasonable estimate of the diffusion coefficient under the appropriate conditions.

Role of apparent diffusion coefficient in intracellular pH gradients

The following are examples of how the apparent diffusion coefficient might influence pH changes within cells. The first example is similar to that given in Irving et al. (1990). We use $D^{app} = 10^{-6}$ cm^2/s and $x^2/4t \simeq D^{app}$ (Crank, 1985). In 2 ms, a pH change will propagate a distance of ~1 μm. Assume that the pH change results from adding proton equivalents through a surface at 3,000 pmol/cm^{2}s for 2 ms. This amount of proton flux is ~100× that supported by the Na/H exchanger of frog skeletal muscle (Abercrombie and Roos, 1983). Using the approximation, flux $\approx D^{app} \Delta C/\Delta X$, the change of the concentration of proton equivalents at the surface, ΔC, is (~3,000 × 10^{-12} mol/cm^{2}s) × (10^{-4} cm)/(10^{-6} cm^2/s) = 0.3×10^{-6} mol/cm^3, or 0.3 mM during the first 2 ms of flux. The local buffering power will determine the actual pH change. If the buffering power in the region were 30 mM, the change in pH would be 0.3 mM/30 mM, or 0.01 pH units after 2 ms of flux and 0.02 U after 8 ms of flux, etc. This change in total proton concentration might be significant for some enzymes located in the region. For example, the activity of the glycolytic enzyme phosphofructokinase may be reduced 10- to 20-fold by a 0.1 pH reduction under certain conditions (Trivedi and Danforth, 1966).

Similar calculations can be made to determine the pH difference between the two ends of an acid-transporting epithelial cell. Assuming an apparent diffusion coefficient of 10^{-6} cm^2/s, a transport of proton equivalents of 500 pmol/cm^{2}s, and a cell length of 25 μm, the difference in the concentration of proton equivalents would be (500 × 10^{-12} mol/cm^{2}s) × (0.0025 cm)/(10^{-6} cm^2 s^{-1}) = 1.25 μmol/cm^3, or 1.25 mmol/liter. With a buffering power of 10 mM, the pH difference would be 0.125 pH units.

APPENDIX

Theory

We shall make the following simplifying assumptions to incorporate hydroxide movement into an expression for the apparent proton diffusion coefficient. (*a*) For simplicity, and because our conclusions are not critically dependent on their exact values, we shall assume the same diffusion coefficient for both hydrogen and hydroxide ions. (We will use a value of 1×10^{-4} cm^2/s in our calculations.)[1] (*b*) Hydrogen ions attach to binding sites on both mobile and immobile molecules within the cell. We shall assume a single mobile buffer species and a single fixed buffer species, although the formulation can easily be extended to more species. (*c*) Movement of hydrogen, hydroxide, and

[1]A chain mechanism, whereby protons jump to, and from, water molecules, accounts for the uniquely rapid movement of both of these ions in water (Bernal and Fowler, 1933; Bockris and Reddy, 1977). Diffusion coefficients calculated from conductance measurements in water (Longsworth, 1954) are 9.3×10^{-5}cm^2/s for the hydronium ion and 5.3×10^{-5}cm^2/s for hydroxide ion.

protonated mobile buffer are independently determined by their concentration gradients. (*d*) The activity coefficients of hydrogen and hydroxide ions are one. (*e*) All species are in chemical equilibrium. (*f*) Hydroxide ions do not attach to either mobile or fixed sites within the cell. The formation of hydroxide-metal ion pairs are considered in the Discussion but is probably of little consequence under our conditions. (*g*) The protonated mobile buffer concentraiton [HM] is linearly dependent on the hydrogen ion concentration [H^+]. This is equivalent to the assumption made by Junge and McLaughlin (1987) that [HM] = $[M]_{tot}[H^+]/K_M$.[2] $[M]_{tot}$ is the total concentration of mobile buffer and K_M is the equilibrium dissociation constant of the mobile buffer. Or, in lieu of assumption *g*, we may assume (*h*) the rate of change of [H^+] with distance is small (d[H^+]/dx must be small enough that certain terms to be identified below are negligible). This is analogous to the assumption made by Irving et al. (1990). Only assumptions *c*, *e*, and *g* or *h* listed above are essential for the mathematical treatment.

Let $\Sigma[H]_i$ and $\Sigma[OH]_j$ represent the sum of concentrations of all forms of H and OH in the system, including the free ions [H^+], [OH^-], and those attached to binding sites. The diffusion equations for [H] and [OH] can be written as described by Junge and McLaughlin (1987) and Irving et al. (1990) and combined to yield the expression:

$$\sum_i \frac{\partial[H]_i}{\partial t} - \sum_j \frac{\partial[OH]_j}{\partial t} = \sum_i D_i \frac{\partial^2[H]_i}{\partial x^2} - \sum_j D_j \frac{\partial^2[OH]_j}{\partial x^2}. \quad \text{(A1)}$$

Formulating the expression as the difference between total hydrogen and hydroxide ions takes into account that the movement of H^+ into an element of volume is equivalent to the removal of OH^- (Grzesiek and Dencher, 1986). If the simplifying assumptions *b* and *f* are made, then

$$\sum[H]_i = [H^+] + [HM] + [HI] \quad \text{(A2)}$$

$$\sum[OH]_j = [OH^-], \quad \text{(A3)}$$

where [HM] and [HI] are the concentrations of the protonated mobile and immobile buffers, respectively. Eq. A1 then becomes:

$$\frac{\partial[H]}{\partial t} - \frac{\partial[OH^-]}{\partial t} + \frac{\partial[HM]}{\partial t} + \frac{\partial[HI]}{\partial t} = D_{H^+}\frac{\partial^2[H^+]}{\partial x^2} - D_{OH^-}\frac{\partial^2[OH^-]}{\partial x^2} + D_M\frac{\partial^2[HM]}{\partial x^2}. \quad \text{(A4)}$$

We consider only distance, *x*, and time, *t*, to be independent variables, and that [HM], [HI], and [OH^-] can be considered as single-valued functions of the parameter [H^+]. This will be true if [HM], [HI], and [OH^-] are in chemical equilibrium with [H^+]. The change in these quantities can be related to the change in [H^+]. Applying the chain rule yields:

$$\frac{\partial[HM]}{\partial t} = \frac{d[HM]}{d[H^+]}\frac{\partial[H^+]}{\partial t} \quad \text{(A5)}$$

and

$$\frac{\partial^2[HM]}{\partial x^2} = \frac{d[HM]}{d[H^+]}\frac{\partial^2[H^+]}{\partial x^2} + \frac{d^2[HM]}{d[H^+]^2}\left(\frac{\partial[H^+]}{\partial x}\right)^2. \quad \text{(A6)}$$

The second term on the right-hand side of Eq. A6 will be negligible as $d^2[HM]/d[H^+]^2$ approaches zero (equivalent to the Junge and McLaughlin assumption), or as $\partial[H^+]/\partial x$ becomes small (analogous to the Irving et al. assumption).

Applying the chain rule to the [OH] terms in Eq. A4 yields:

$$\frac{\partial[OH^-]}{\partial t} = \frac{d[OH^-]}{d[H^+]}\frac{\partial[H^+]}{\partial t} \quad \text{(A7)}$$

$$\frac{\partial^2[OH^-]}{\partial x^2} = \frac{d[OH^-]}{d[H^+]}\frac{\partial^2[H^+]}{\partial x^2} + \frac{d^2[OH^-]}{d[H^+]^2}\left(\frac{\partial[H^+]}{\partial x}\right)^2. \quad \text{(A8)}$$

It can be easily shown that $d[OH^-]/d[H^+] = -(10^{-14}[H^+]^{-2})$ and $d^2[OH^-]/d[H^+]^2 = (2 \times 10^{-14}[H^+]^{-3})$. The second terms on the right-hand side of Eqs. A6 and A8 will be negligible if $\partial[H^+]/\partial x$ is small (assumption of Irving et al., 1990). $\partial[H^+]/\partial x$ is expected to become smaller at alkaline pH or as the pH deflections become smaller. Also, the second term in Eq. A8 is small if [H^+] is large, i.e., at very acidic values of pH where $2 \times 10^{-14}[H^+]^{-3}$ is small. If the second terms in Eqs. A6 and A8 are neglected, and the expressions A5, A6, A7, and A8 are substituted into Eq. A4, then a one-dimensional diffusion equation results in which $\partial[H^+]/\partial t$ is related to $\partial^2[H^+]/\partial x^2$. This produces an equation analogous to that derived by Junge and McLaughlin (1987) and Irving et al. (1990), in which an apparent diffusion coefficient can be defined as:

$$D^{app} = \frac{D_{H^+} + \Phi D_{OH^-} + D_M d[HM]/d[H^+]}{1 + \Phi + d[HM]/d[H^+] + d[HI]/d[H^+]}, \quad \text{(A9)}$$

where $\Phi = (10^{-14}[H^+]^{-2})$.

If $D_{H^+} = D_{OH^-} = D_{H^{+-}}$ (assumption *a*), then

$$D^{app} = \frac{D_{H^{+-}}(1 + \Phi) + D_M d[HM]/d[H^+]}{1 + \Phi + d[HM]/d[H^+] + d[HI]/d[H^+]}. \quad \text{(A10)}$$

For acidic values of pH, $(1 + \Phi) \approx 1$; at neutral pH, $(1 + \Phi) = 2$; and for alkaline pH, $(1 + \Phi)$ becomes large. Thus, at alkaline pH, according to this model, the apparent diffusion coefficient may be influenced by $D_{H^{+-}}$, i.e., hydroxide movement. This happens if $D_{OH^-} \cdot \Phi$ becomes comparable in magnitude to the term $D_M \cdot d[HM]/d[H^+]$. (See Eq. 7 in the Discussion.)[3]

Using a series of steps analogous to those outlined above (Eqs. A1–A10), but with the quantity [OH^-] or the quantity $[H^{+-}] = [H^+] - [OH^-]$ in place of [H^+], leads to an identical expression for the apparent diffusion coefficient. Therefore, we believe we are justified in using $[H^{+-}]$ to calculate D^{app}. The numerical calculations of apparent diffusion coefficients shown in Fig. A2 were made using the quantity $[H^{+-}]$. Their convergence, for small jumps of pH, to Eq. A10 is an additional confirmation of the validity of using $[H^{+-}]$.

[2]The assumption that [HM] depends linearly on [H^+] is an approximation of the equilibrium binding equation for values of [H^+] $\ll K$. It should be noted, however, that the slope of the curve of [HM] versus [H^+] is always decreasing as [H^+] rises, even at the lowest values of [H^+].

[3]For an open buffer system of CO_2/HCO_3^-, d[HM]d[H^+] is equivalent to $-d[HCO_3^-]/d[H^+] = K_M[H_2CO_3]/H^+]^2$. At 5% CO_2, pH 7, $K_M[H_2CO_3]/[H^+]^2 = 9.5 \times 10^4$. Compare with Table 3.

The factor d [HM]/d [H^+] can be related to the buffering power, β_M, of the mobile buffer or to its chemical properties (Junge and McLaughlin, 1987; Irving et al., 1990):

$$\frac{d[HM]}{d[H^+]} = \frac{\beta_M}{[H^+]\ln 10} \leq \frac{[M]_{tot}}{K_M} \quad (A11)$$

$$\frac{d[HI]}{d[H^+]} = \frac{\beta_I}{[H^+]\ln 10} \leq \frac{[I]_{tot}}{K_I}, \quad (A12)$$

where $[M]_{tot}$ and $[I]_{tot}$ are the total concentrations of the mobile and immobile buffers and K_M and K_I are their equilibrium dissociation constants. If the buffering power β were constant, then the terms d [HM]/d [H^+] and d [HI]/d [H^+] would vary as $1/[H^+]$.

In the following, m = d [HM]/d [H^+] and i = d [HI]/d [H^+]. These dimensionless parameters represent the change of protonated mobile (m) or immobile (i) buffer concentration for a change in concentration of free protons. For simplicity in the calculations, we will assume constant parameters, i.e., assumption of Junge and McLaughlin (1987). Eqs. A11 and A12 show how these parameters are related to buffering power, etc. Table 3 gives maximum values of m for some typical mobile pH buffers and the values of these parameters at different pH. In that table, the three amino acids are the constituents of the standard buffer solution that we used to make the "artificial axoplasm."

Fig. A1 shows, assuming m and i are constant according to Eq. A10, the predicted effects of the mobile buffer factor, m, the immobile buffer factor, i, and the pH on the diffusion coefficient. If $m \gg i$, then

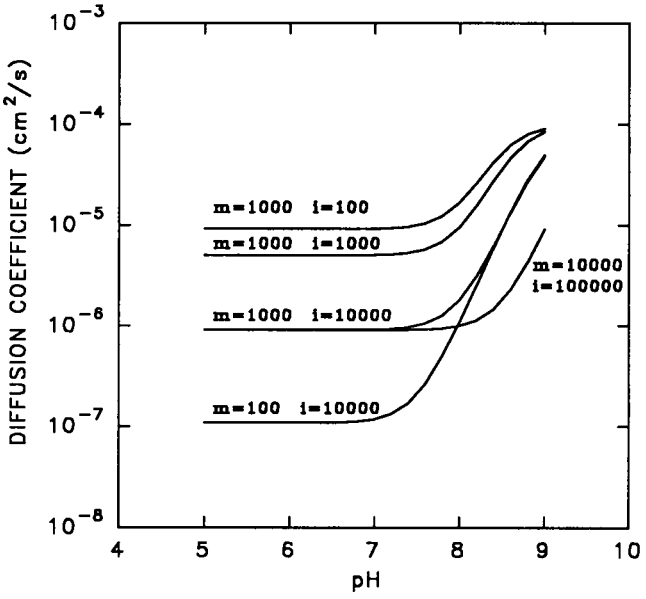

FIGURE A1 Theoretical effects of the mobile buffer (m), immobile buffer (i), and pH on the apparent diffusion coefficient. m = d [HM]/d [H^+] and i = d [HI]/d [H^+]. The diffusion coefficient of the mobile buffer is taken as 10^{-5} cm^2/s and that of protons and hydroxide as $10^{-4}cm^2/s$. At alkaline pH, hydroxide ion movement dominates in the expression for the diffusion coefficient because m and i are assumed constant. The amount of immobile buffer relative to the amount of mobile buffer determines how far the apparent diffusion coefficient will drop below that of the mobile buffer at acidic pH.

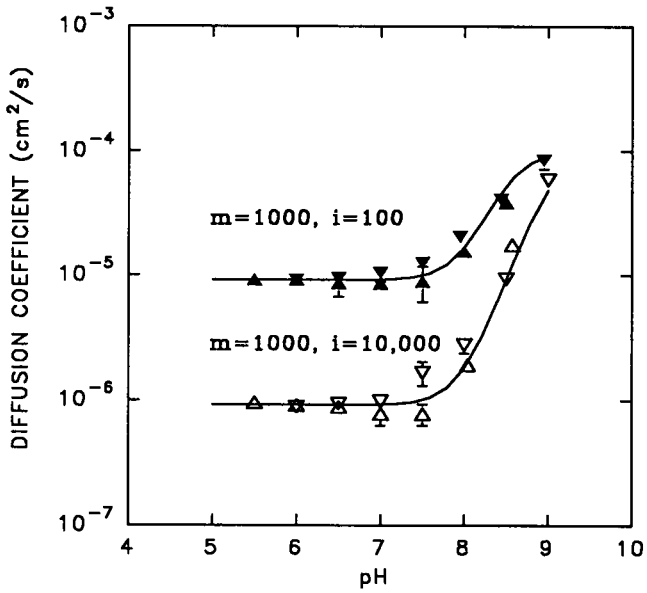

FIGURE A2 Numerical check of the theoretical expression for the diffusion coefficient. The symbols represent values determined by finite difference calculations (see Methods). In these calculations, the mobile buffer had an equilibrium dissociation constant, K_d, of 10^{-4} M and a concentation of 0.1 M. The immobile buffer had a K_d of 10^{-4} M and concentrations of 0.01 M (*filled triangles*) or 1 M (*open triangles*). In the numerical simulation, the basal pH was varied from 5.5 to 9.0 in 0.5-U increments. The pH was deflected 0.5 U from the basal value in the acidic direction (downward pointing triangles) or 0.5 U in the alkaline direction (*upward pointing arrows*). The diffusion coefficients were then calculated from the relaxation of the concentration profile. The lines are from Eq. A10, using the same parameters as in the numerical calculations.

the expected diffusion coefficient will be dominated by the mobile buffer. In general, the ratio of the factor m to the factor i determines the amount that the diffusion coefficient drops below that of the mobile buffer. The sum of m plus i determines the pH at which the diffusion coefficient begins to rise toward the value for hydroxide ions, i.e., the bend in the curve. Because we have assumed that m and i are constant (Junge and McLaughlin, 1987), the hydroxide term in Eq. A9 begins to dominate at alkaline pH in Fig. A1. The reason that hydroxide does not contribute significantly to the apparent diffusion coefficient in *Myxicola* is that the sum of $m + i$ in *Myxicola* at pH 8 is $\sim 10^6$, which is an order of magnitude higher than the highest values shown in Fig. A1 ($m = 10^4, i = 10^5$).

In order to explore the regions in which the neglect of the second terms on the right-hand side of Eqs. A6 and A8 are justified, we calculated the diffusion coefficients, with mobile and immobile buffers present, using the finite difference approach described in the Methods. The results for both acidic and alkaline pH jumps with a buffer pK = 4 are shown in Fig. A2. Although not shown on the figure, the deviation of the numerically determined diffusion coefficient from that predicted by the analytical equation (A10) became larger for larger pH jumps. For example, with 1 M immobile buffer concentration, deflections from pH 7.5 to 7.4 gave a numerically-determined diffusion coefficient of 1.1×10^{-6} cm^2/s, while deflections to pH 5 gave an average of 2.1×10^{-6} cm^2/s. In the example shown in the Fig. A2, the pH deflections were 0.5 U in either direction.

The numerical simulations revealed higher values for the effective diffusion coefficient for acidic jumps than for alkaline jumps. This feature required the presence of a mobile buffer. Without a mobile buffer, the acidic pH jumps gave a slightly lower diffusion coefficient than the alkaline jumps. At alkaline pH, the diffusion coefficient approached that of hydroxide.

We thank Drs. P. L. Becker, W. K. Chandler, R. B. Gunn, and J. W. Nichols for constructive comments on earlier versions of this manuscript.

Supported by NIH grant NS-19194.

Received for publication 26 July 1991 and in final form 20 January 1992.

REFERENCES

Abercrombie, R. F. 1988. Hydrogen and calcium ion diffusion in axoplasm. *In* Microcompartmentation. D. P. Jones, editor. CRC Press, Inc., Boca Raton, Fl. 209–225.

Abercrombie, R. F., and C. E. Hart. 1986. Calcium and proton buffering and diffusion in isolated cytoplasm from *Myxicola* axons. *Am. J. Physiol.* 250 (*Cell Physiol.* 19):C391–C405.

Abercrombie, R. F., and A. Roos. 1983. The intracellular pH of frog skeletal muscle: its regulation in hypertonic solutions. *J. Physiol.* 345:189–204.

Aw, T. Y., and D. P. Jones. 1988. Microzonation of ATP and pH in the aqueous cytoplasm of mammalian cells. *In* Microcompartmentation. D. P. Jones, editor. CRC Press, Inc., Boca Raton, FL. 191–204.

Baker, P., and W. Schlaepfer. 1978. Uptake and binding of calcium by axoplasm isolated from giant axons of *Loligo* and *Myxicola*. *J. Physiol.* 276:103–125.

Bernal, J. D., and R. H. Fowler. 1933. A theory of water and solutions, with particular reference to hydrogen and hydroxyl ions. *J. Chem. Phys.* 1:515–548.

Bockris, J. O'M., and A. K. N. Reddy. 1977. Modern Electrochemistry, Vol. 1. Plenum Press, New York. 622 pp.

Boron, W. F., and P. De Weer. 1976. Intracellular pH transients in squid giant axons caused by CO_2, NH_3, and metabolic inhibitors. *J. Gen. Physiol.* 67:91–112.

Boron, W. F., W. C. McCormick, and A. Roos. 1979. pH regulation in barnacle muscle fibers: dependence on intracellular and extracellular pH. *Am. J. Physiol.* 237:C185–C193.

Bowen, W., and H. Martin. 1964. The diffusion of adenosine triphosphate through aqueous solutions. *Arch. Biochem. Biophys.* 107:30–36.

Crank, J. 1985. The Mathematics of Diffusion. Clarendon Press, Oxford. 37: 139–142.

Dawson, R., D. Elliott, W. Elliott, and K. Jones. 1986. Data for Biochemical Research. Clarendon Press, Oxford. 580 pp.

De Weer, P. 1976. Axoplasmic free magnesium levels and magnesium extrusion from squid giant axons. *J. Gen. Physiol.* 68:159–178.

Edwards, O. W., R. L. Dunn, J. D. Hatfield, E. O. Huffman, and K. L. Elmore. 1966. Diffusion at 25° of solutions in the system phosphoric acid-monocalcium phosphate-water. *J. Phys. Chem.* 70:217–226.

Gilbert, D. S. 1975. Axoplasm chemical composition in *Myxicola* and solubility properties of its structural proteins. *J. Physiol.* 253:303–319.

Grzesiek, S., and N. A. Dencher. 1986. Dependency of pH relaxation across vesicular membranes on the buffering power of bulk solutions and lipids. *Biophys. J.* 50:265–276.

Irving, M., J. Maylie, N. L. Sizto, and W. K. Chandler. 1990. Intracellular diffusion in the presence of mobile buffers. Application to proton movement in muscle. *Biophys. J.* 57:717–721.

Junge, W., and S. McLaughlin. 1987. The role of fixed and mobile buffers in the kinetics of proton movement. *Biochim. Biophys. Acta.* 890:1–5.

Longsworth, L. 1954. Temperature dependence of diffusion in aqueous solutions. *J. Phys. Chem.* 58:770–773.

Martell, A., and R. Smith. 1974. Critical stability constants, Vol. 1. Amino Acids. Plenum Press, New York. 486 pp.

Mason, C. M., and J. B. Culvern. 1949. Electrical conductivity of orthophosphoric acid and of sodium and potassium dihydrogen phosphates at 25°C. *J. Am. Chem. Soc.* 71:2387–2393.

McBain. M. 1944. Diffusion of the lower alkyl sulfonic acids and some large molecules. *J. Phys. Chem.* 48:237–241.

Roos, A., and W. F. Boron. 1981. Intracellular pH. *Physiol. Rev.* 61:296–434.

Smith, R. M., and A. E. Martell. 1981. Critical Stability Constants, Vol. 4. Inorganic Complexes. Plenum Press, New York. 272 pp.

Spyropoulos, C. 1960. Cytoplasmic pH of nerve fibres. *J. Neurochem.* 5:185–194.

Trivedi, B., and W. H. Danforth. 1966. Effect of pH on the kinetics of frog muscle phosphofructokinase. *J. Biol. Chem.* 241:4110–4112.